

OPTIMIZED NULL STEERING IN COMPACT BOWTIE ANTENNA ARRAY USING SIMULATION DRIVEN TAGUCHI METHOD

Baljinder Kaur, Anupma Marwaha

Sant Longowal Institute of Engineering and Technology, Electronics and Communication Engineering Department, Longowal, Punjab, India-148106 (✉ baljinderkaursidhu@rediffmail.com, +91 94 6429 2719, marwaha_anupma@yahoo.co.in)

Abstract

Ever rising increase in number of wireless services has prompted the use of spatial multiplexing through null steering. Various algorithms provide electronic control of antenna array pattern. Simulation-driven technique further introduces correction in array factor to account for array geometry. Taguchi method is used here to combat interference in practical antenna arrays of non-isotropic elements, by incorporating the effect of antenna element pattern on array pattern control in the optimization algorithm. 4-element rectangular and bowtie patch antenna arrays are considered to validate the effectiveness of Taguchi optimization. The difference in the computed excitations and accuracy of null steering confirms the dependence of beam pattern on element factor and hence eliminates the need for extra computations performed by conventional algorithms based on array factor correction. Taguchi method employs an orthogonal array and converges rapidly to the desired radiation pattern in 25 iterations, thus signifying it to be computationally cost-effective. A higher gain and a significant reduction in *side lobe level* (SLL) was obtained for the bowtie array. Further, due to feed along parallel edges of the patch, the radiating edges being slanted to form the bow shape results in a significant reduction in the area as compared with the rectangular patch designed to resonate at the same frequency.

Keywords: interference suppression, non-isotropic antenna array, mutual coupling, simulation-controlled optimization, Taguchi method.

© 2020 Polish Academy of Sciences. All rights reserved

1. Introduction

The wireless communication services are emerging at an extensive rate. As the communication systems have evolved and grown in complexity, the number of unwanted directional interferences increased resulting in degradation of the system performance. Thus, interference suppression by controlling the radiation pattern of an antenna through orientation of the nulls towards the direction of interference is a vital issue [1, 2] to meet the requirements of expanding wireless communication through spatial division multiple access.

In the recent years, different optimization techniques have been explored for null steering of an antenna array of isotropic elements by computing array excitations in different ways to control the pattern, but have been less explored for null steering of arrays of non-isotropic elements [3, 4]. There are various key issues that need to be addressed in designing the non-isotropic antenna arrays. The first and foremost is the trade-off between the directivity and the side lobe level. A compact antenna array with high directivity and low side lobe level can enhance the reliability and validity of a communication system [5]. Another vital issue is the presence of mutual coupling between the array elements. The mutual coupling results in non-ideal element excitations which have detrimental effects on the implementation of the pattern synthesis techniques as compared with that of isotropic arrays [6]. The element excitations become interdependent since the excitation of one element is affected by that of the surrounding elements. Thus, the input impedance of the elements becomes scan-dependent, resulting in impedance mismatch. Depending on the feed network, the reflected signals may enter the input terminals of the surrounding elements which causes further excitation errors [7]. Hence, it is apparent that for efficient electronic steering of the pattern by virtue of controlling the excitations it is required to meet the above challenges in the design of non-isotropic antenna array. The metaheuristic optimization techniques such as genetic algorithm, particle swarm optimization, simulated annealing, chicken swarm optimization *etc.* are useful for array pattern synthesis but they need hundreds and even thousands of objective function calls. Thus, they are applicable to problems where the array evaluation cost is not of concern [8]. In the recent years simulation-controlled optimization is considered for non-isotropic antenna arrays and a correction factor is introduced in the array factor to account for the antenna element geometry [9, 10]. For simulation-driven optimization of non-isotropic antenna arrays, the convergence rate of the optimization technique has a significant effect on the computational cost as every iteration is followed by complete simulation of the array structure and thus, processing time rises with each iteration. Hence, in order to achieve the targeted pattern at a faster rate, the Taguchi optimization has been applied here as it requires only a small fraction of all possible parameter-level combinations based on the theory of fractional orthogonal arrays [11]. Moreover, due to the inherent feature of Taguchi method to account for the element factor through the set of measurements, there is no need to add a correction factor, thus avoiding the extra computations.

Liang *et al.* [4] have employed Cuckoo Search-Chicken Swarm Optimization algorithm for side lobe suppression of linear and circular antenna arrays of different number of elements and a simulative analysis is performed on a 4-element linear rectangular patch antenna array. In [4] all the results are presented for isotropic antenna arrays ignoring the effects of element factor. The present work accounts for the element factor of a non-isotropic antenna element through simulation-driven optimization. The effectiveness of null steering techniques for non-isotropic geometries is initially demonstrated by applying Schelkunoff polynomial method. A compact bowtie patch antenna is designed in this work and the patch size is effectively reduced by using parallel edges of the structure for feeding. When embedded in an array, the small size of bowtie patch results in a larger edge-to-edge spacing between the adjacent elements for inter-element spacing of half wavelength. The larger spacing reduces the mutual coupling effect, thus avoiding the deterioration of radiation pattern due to the mutual coupling. Taguchi Optimization is then applied to steer the nulls of 4-element non-isotropic arrays of rectangular and bowtie patches. The resultant patterns obtained by applying both the methods are then analysed for comparison of accuracy and resolution of null steering thus achieved.

2. Array synthesis

Assuming that the antenna array comprises identical antenna elements oriented in the same direction, the beam pattern $B(\theta)$ [12] of an equi-spaced linear antenna array can be expressed as the product of an array factor $AF(\theta)$ and an element factor $EF(\theta)$:

$$B(\theta) = AF(\theta) \times EF(\theta). \quad (1)$$

The element factor corresponds to the gain of the elementary antennas and, for an N -element linear array shown in Fig. 1, the array factor is expressed as:

$$AF(\theta) = \sum_{n=0}^{N-1} I_n e^{\frac{jn2\pi d}{\lambda} \sin(\theta)}, \quad (2)$$

where I_n is the amplitude of current fed to the n th element; d is the spacing between the elements and θ is the angle of incidence with respect to the array normal.

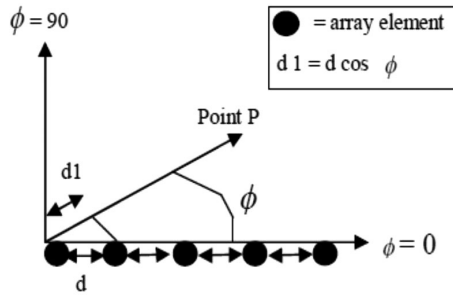


Fig. 1. Geometry of a linear antenna array of N isotropic elements.

For analytical reasons, the simplification $EF = 1$ assuming the elementary radiators to be isotropic, is commonly applied to replace (1) by (2). Substituting $\psi = \frac{2\pi d}{\lambda} \sin(\theta)$ then yields [12]:

$$AF(\psi) = \sum_{n=0}^{N-1} I_n e^{jn\psi}. \quad (3)$$

Equation (3) is an expression for the array factor in terms of the frequency-dependent variable ψ . The element factor $EF(\theta)$ or the array factor $AF(\theta)$ can be used to control the radiation pattern of an array. It is therefore important to model the array taking into account the element factor, *i.e.* the active element patterns, to predict the mutual coupling effect while implementing pattern synthesis for non-isotropic antenna arrays. The array factor depends on the amplitude, phase, position and number of elements. However, in practice the position is not varied and it is tried to steer the radiation pattern only by controlling the complex current excitations on the antenna elements. Null steering by amplitude control has been considered in this work to avoid the non-linearities and approximations present in phase-control null steering methods, as mentioned in [13]. The phase-only nulling method is inherently non-linear and thus cannot be solved by analytical methods without any approximation. Moreover, it has been observed in [14] that the nulls and the side lobe level in an array are more sensitive to random errors caused by the equipment used, in the element phase excitations as compared with the amplitude excitations.

3. Null steering using Schelkunoff polynomial method

The *Schelkunoff polynomial method* (SPM) is based on solving the governing (2) for computing element excitations corresponding to a desired pattern by employing the normalized expression for the electric field strength with an assumption of element factor being equal to unity. The method calculates the element excitations for a desired null-controlled pattern for a given number and angular orientation of the nulls.

3.1. Antenna array of isotropic elements

The radiation pattern of a 4-element isotropic antenna array fed with a uniform excitation has nulls at 60° and -60° , and interference along 50° , -50° and 130° , as shown in Fig. 2a. The excitation ratio as computed using the MATLAB code developed for SPM to steer three nulls towards 50° , -50° and 130° is $1:1.5826:1.5826:1$ which when normalized, becomes $0.6318:1:1:0.6318$. As depicted from the 2D radiation patterns of a 4-element isotropic antenna array shown in Fig. 2b, accurate steering of nulls along 50° , -50° and 130° is achieved for an isotropic antenna array using SPM.

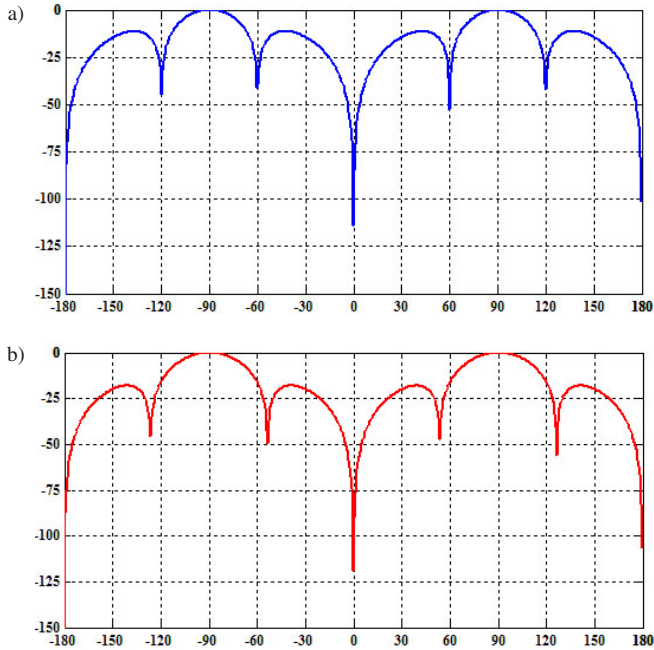


Fig. 2. a) 2D Radiation patterns for a 4-element isotropic antenna array with uniform excitations; b) a pattern with nulls imposed at 50° , -50° and 130° .

3.2. Antenna array of rectangular patches

The CPW-fed rectangular patch with dimensions given in Table 1 has been designed using a 1.6 mm thick FR4 substrate with a relative dielectric constant 4.4 and a loss tangent 0.02. The 50 ohm CPW transmission line has been designed with a metal strip width $2a = 1.8$ mm and a gap dimension of 0.22 mm calculated using the equations given in [15]. The radiation pattern

of a rectangular patch antenna shown in Fig. 4 appears to be a broad-directional pattern and has consequently a low directivity. A higher directivity for making the radiation pattern narrower, and electronic control of the radiation pattern through excitations can be achieved by employing antenna arrays, as shown in Fig. 3. Initially, the elements of the array with an inter-element

Table 1. Dimensions of a rectangular patch antenna.

Length of rectangular patch (L)	14.06 mm
Width of rectangular patch (W)	18.6 mm
Area	261.52 mm ²
L_g	12.9 mm
W_g	8.18 mm

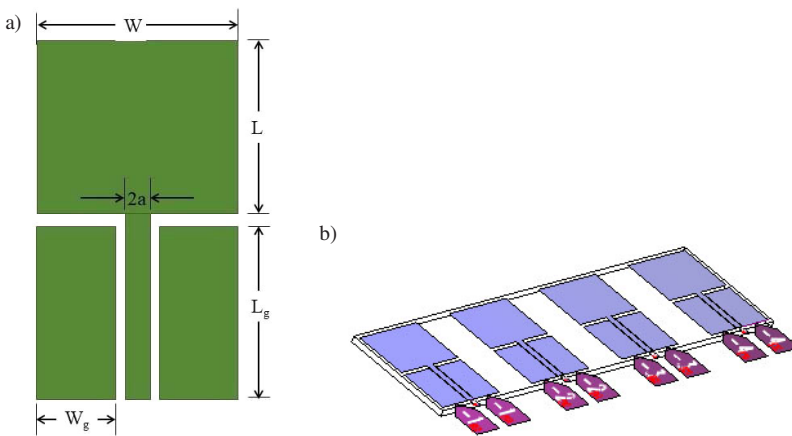


Fig. 3. a) A rectangular patch; b) IE3D model of a 4-element rectangular patch antenna array.

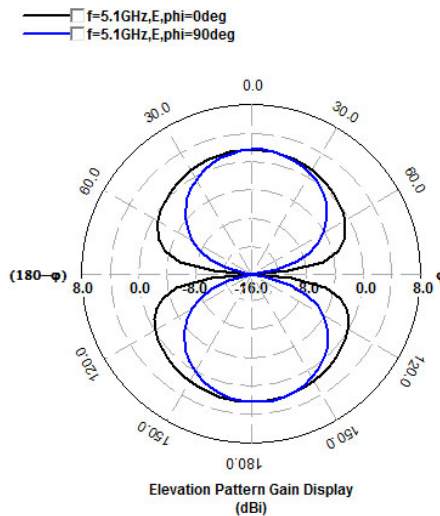


Fig. 4. The radiation pattern of a rectangular patch antenna.

spacing of $\lambda/2$, i.e. 29.1 mm, are excited with uniform amplitudes, and generate the radiation pattern shown in Fig. 7a and Fig. 10, having side lobes present along 45° and -45° with SLL of -11.96 dB and -11.95 dB, respectively. Nulls are present along 30° , -30° and 150° with NDL of -19.21 dB, -19.1 dB and -18.81 dB, respectively.

The element excitations 0.6318:1:1:0.6318 obtained using SPM to steer the nulls towards 50° , -50° and 130° when fed to a 4-element rectangular patch antenna array result in the radiation pattern shown in Fig. 7b and Fig. 10, with the nulls steered to -36° , 144° and 36° which are deviated from the desired direction. Rather, the directions along which the nulls are targeted to be steered, carry strong interference with side lobes present along 50° and -50° with a side lobe level of -16.99 dB. It can therefore be interpreted from the results achieved in Fig. 7b and Fig. 10 that the SPM excitations when applied to rectangular patches do not generate a pattern with nulls steered to desired angular positions due to the element pattern and excitation errors owing to the coupling effect between the rectangular patches.

3.3. Antenna array of bowtie patches

The bowtie patch of dimensions as shown in Table 2 is designed and simulated using IE3D. Focusing on a low-profile antenna design, the size requirement of the bowtie patch is reduced by moving the feed along the parallel edges of the bowtie patch and the slant edges are made to radiate. Fig. 6 depicts the broad sided radiation pattern of the bowtie patch antenna with radiation falling to zero along the axis of the patch.

Table 2. Dimensions of a bowtie patch antenna (mm).

$L'/2$	W'	W_C	S	Area	L'_g	W'_g
7.07	10	1.0	10	55	8	2.88

A 4-element non-isotropic antenna array shown in Fig. 5 has been designed using a bowtie patch as the elementary radiator with a distance of $\lambda/2$, i.e. 29.1 mm, between the elements. The elements of the array are initially excited uniformly through coplanar waveguide feeding.

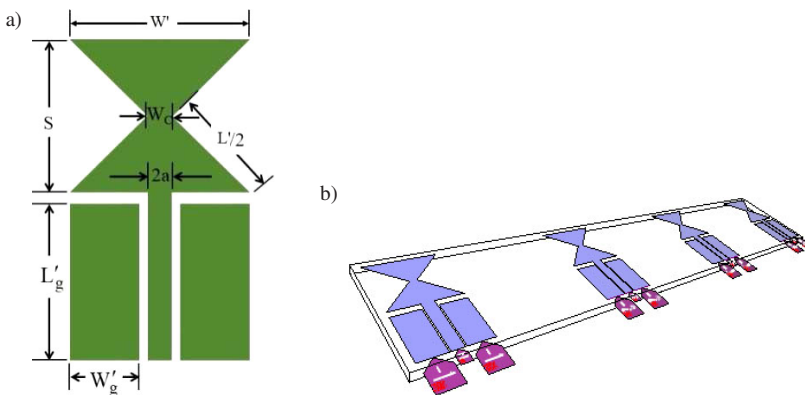


Fig. 5. a) A bowtie patch; b) IE3D model of a 4-element bowtie patch antenna array.

The radiation pattern of the uniformly excited bowtie antenna array as shown in Fig. 8a and Fig. 10 exhibits nulls along 30° , -30° and 150° with null depth levels of -22.59 dB,

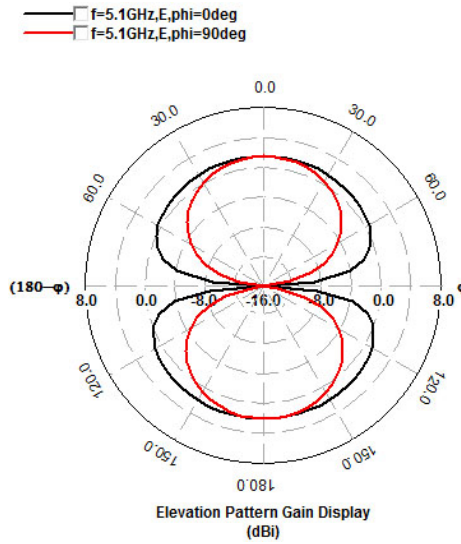


Fig. 6. The radiation pattern of a bowtie patch antenna.

-22.59 dB and -22.16 dB, respectively, and side lobes are present at 45° and -45° with SLL of -13.31 dB. The excitation of the elements with weights 0.6318, 1, 1 and 0.6318, as computed using SPM results in steering the nulls towards 34.71° , -34.71° and 145.28° with ND -26.68 dB, -26.68 dB and -26.27 dB, as shown in Fig. 10. For a bowtie antenna array, the element size is comparatively less than that of a rectangular antenna resonating at almost the same frequency. The reduced size of the bowtie element facilitates large edge-to-edge spacing between the adjacent elements with a reduced coupling effect. It can be seen from Fig. 8b and Fig. 10 that even for a bowtie antenna array having a less coupling effect as compared with a rectangular antenna array, the nulls are not accurately steered to 50° , -50° and 130° .

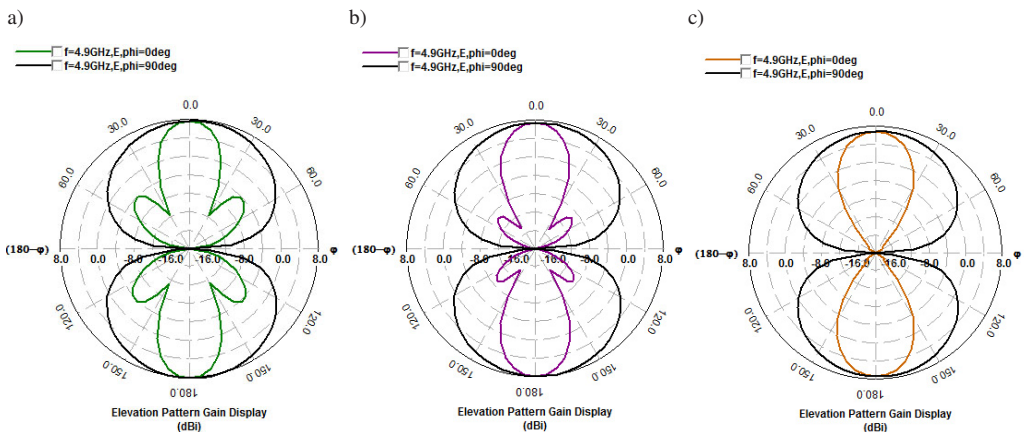


Fig. 7. 2D radiation patterns for a 4-element rectangular patch antenna array using different excitations. a) Uniform excitation; b) SPM; c) optimized using Taguchi method.

However, the nulls are steered towards 35° , -35° and 145° with side lobes present at 50° and -50° , when applied with SPM weights. For efficient null steering in non-isotropic antenna arrays, it is thus required to take into account the effect of element geometry and mutual coupling on radiation patterns. Schelkunoff polynomial method is based only on the array factor and does not consider the element factor. The weights calculated for steering nulls in an isotropic antenna array need to be modified to incorporate the excitation errors resulting from the coupling effect present in non-isotropic antenna arrays. Thus, there arises a need to compute and optimize the weights required for steering the nulls in a non-isotropic antenna array.

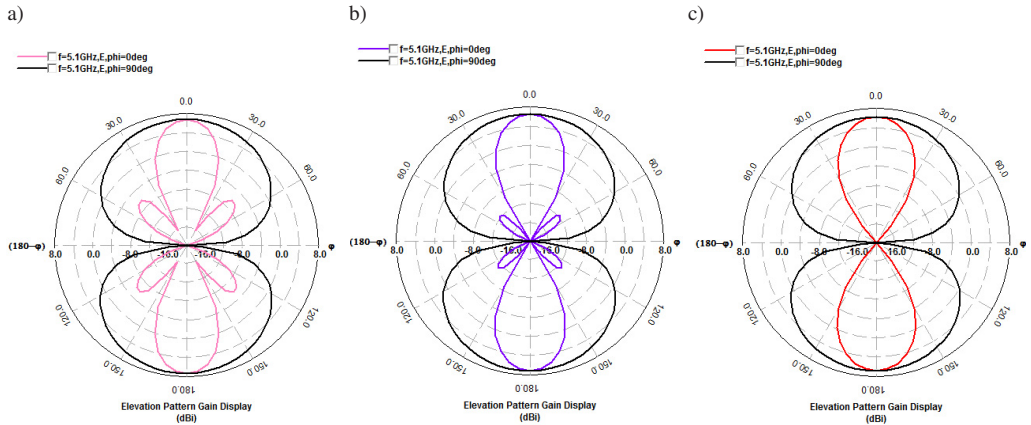


Fig. 8. 2D radiation patterns for a 4-element bowtie patch antenna array using different excitations. a) Uniform excitation; b) SPM; c) optimized using Taguchi method.

4. Taguchi optimization technique for generating null controlled patterns

The optimization procedure based on Taguchi method starts with selecting an orthogonal array and defining an appropriate fitness function. The method employs orthogonal arrays to decrease the test trials to be performed while optimization, thus reducing the excessive computational loads present in simulation-driven optimization. The various parameters of an orthogonal array, such as the number of experiments and levels, are decided from the number of factors to be optimized. MATLAB code has been developed to implement Taguchi method as an external optimizer in IE3D and to access the IE3D engine in order to optimize the element excitations to generate a null-controlled pattern through simulation-driven optimization. The tasks performed by the optimization code are to extract the data from the IE3D engine in order to determine a pre-defined fitness function and then to replace the excitations in the .sim file with the values corresponding to the level values of the current iteration till the termination criteria is met and the optimized excitations are achieved. The initial values of element excitations are selected in a range (0–1) and saved in .sim file and are changed after each experiment by the algorithm. The simulated results saved in .patt file by IE3D are accessed using MATLAB code so as to calculate the fitness function and S/N ratio corresponding to all the experiments of the orthogonal array. The element excitations are then optimized by computing the response table. The simulation-driven optimization is carried out using the in-house interface between the IE3D EM solver and Taguchi optimization algorithm implemented in MATLAB. The flowchart shown in Fig. 9 summarizes the implementation of Taguchi method.

4.1. Optimized null steering in antenna array of rectangular patches

For the 4-element rectangular antenna array shown in Fig. 3, it is desired to optimize the element excitations using Taguchi method so that the radiation pattern has nulls at 50° , -50° and 130° . Because of the symmetry followed by the element excitations, the excitation magnitudes of 2 elements are optimized in a range (0–1) by selecting an L_9 orthogonal array with three levels taken as 0.25, 0.5 and 0.75, as shown in Table 3. The initial level difference (LD_1) is taken to be 0.25 and the subsequent level differences for the higher iterations are computed by taking a reduction rate (RR) of 0.75 till the termination criterion is met, i.e. $LD_i/LD_1 <$ the converged value. LD_i represents the level difference for the i -th iteration and the converged value taken here is 0.001.

$$\text{Fitness} = \text{Min} \left[\sum \left(\theta_{\text{null}}^K - \theta_{\text{Etotal min}}^{\text{FR}} \right) \right], \quad (4)$$

$$S/N = -20 \log(\text{Fitness}) \text{ dB}. \quad (5)$$

Table 3. L_9 orthogonal array for 1st iteration (rectangular antenna array).

Experiment	Element 1	Element 2	Fitness	S/N Ratio (dB)
1	1	1	19.76	-59.6732
2	1	2	9.68	-45.4012
3	1	3	0.4	18.3258
4	2	1	25.8	-65.0075
5	2	2	19.76	-59.6732
6	2	3	14.72	-53.7841
7	3	1	24.6	-64.0549
8	3	2	25.6	-64.8518
9	3	3	19.76	-59.6732

Table 4 presents the values of fitness functions and corresponding S/N ratios for each experiment of the first iteration, computed using (4) and (5). After performing all the experiments of 1st iteration, the average S/N ratio for every level m of each parameter n is then calculated using (6) and is used to build a response table shown in Table 4 and the optimum levels are identified from the largest value of average S/N ratio corresponding to each element.

Table 4. A response table for a rectangular antenna array.

Element/Level	1	2
1	-28.9162	-62.9119
2	-59.4883	-56.6421
3	-62.86	-31.7105
$ \eta_{\text{max}} - \eta_{\text{min}} $	33.9438	31.2014
Ranking	1	2

In the first iteration the optimal level for element 1 corresponding to the maximum S/N average of -28.9162 is level 1, i.e. 0.25, and for element 2 it is level 3, i.e. 0.75, corresponding

to the maximum S/N average of -31.7105 dB, as interpreted from Table 4. The optimal levels of 0.25 and 0.75 are taken as the values for level 2 for elements 1 and 2, respectively, for 2nd iteration. The levels 1 and 3 are thus, computed by adding the level difference LD_2 , i.e. 0.1875, obtained from (7).

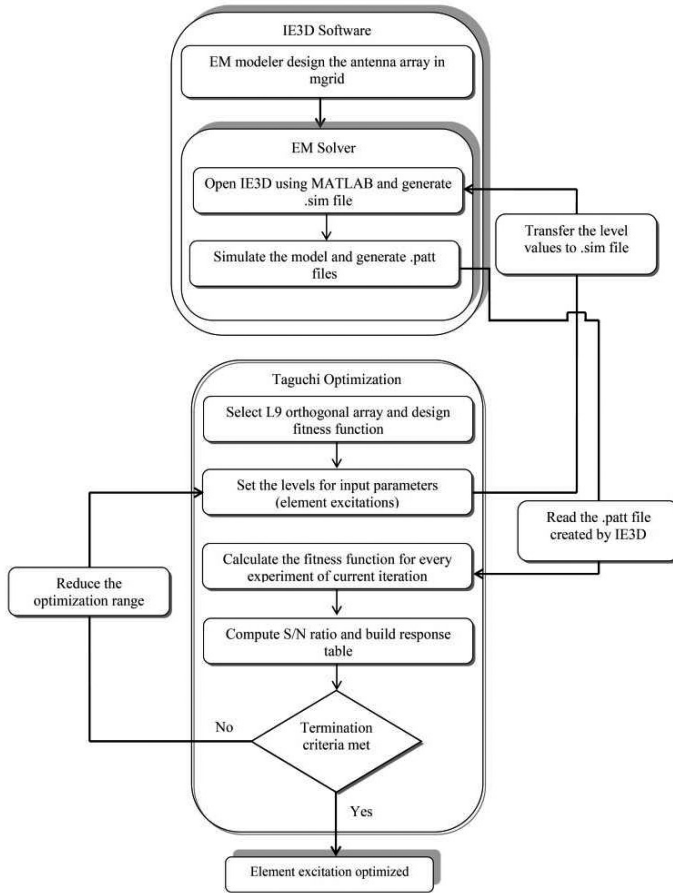


Fig. 9. A flow chart of executing Taguchi Method as an external optimizer in IE3D through interfacing.

$$\left(\frac{S}{N}\right)_{average}(m, n) = \frac{1}{N} \sum_{i, OA(i, n)=m} \left(\frac{S}{N_i}\right), \quad (6)$$

$$LD_{i+1} = (RR)(LD_i) = \left(RR^i\right)(LD_1) = RR(i)LD_1. \quad (7)$$

Optimized excitations thus obtained by applying Taguchi method to null steering are 0.2097, 0.5906, 0.5906 and 0.2097 with normalized amplitudes of 0.355, 1, 1 and 0.355 for the 4 elements of the array, as mentioned in Table 5.

The resultant pattern has been obtained after 25 iterations, with nulls steered exactly towards 50° , -50° and 130° , as shown in Fig. 7c and Fig. 10, with a significant drop achieved in the null depth level, i.e. -25.01 dB, -24.95 dB and -24.71 dB, respectively. Moreover, the side lobes are also suppressed to a greater extent with SLL of -24 dB.

Table 5. Optimized excitations obtained using Taguchi to steer nulls to -50° , 50° and 130° for a rectangular patch antenna array.

Element position	1	2	3	4
Amplitude	0.2097	0.5906	0.5906	0.2097
Normalized Amplitude	0.355	1	1	0.355

4.2. Optimized null steering in antenna array of bowtie patches

The bowtie antenna array shown in Fig. 5 is then considered for steering nulls in the radiation pattern by employing Taguchi optimization technique. The excitations of two elements of the designed 4-element bowtie antenna array have been optimized in a range (0–1) to steer the nulls at 50° , -50° and 130° . Thus, an L_9 orthogonal array with 2 factors and 3 levels has been selected and the corresponding fitness and S/N ratio values as computed during the first iteration are shown in Table 6.

Table 6. An L_9 orthogonal array (Bowtie antenna array).

Experiment	Element 1	Element 2	Fitness	S/N Ratio (dB)
1	1	1	19.64	-59.5514
2	1	2	9.50	-45.0258
3	1	3	0.50	13.8629
4	2	1	25.50	-64.7736
5	2	2	19.64	-59.5514
6	2	3	15.14	-54.3468
7	3	1	25.00	-64.3775
8	3	2	25.05	-64.4175
9	3	3	19.64	-59.5514

Table 7 presents a response table for 1st iteration and the differences between the maximum and minimum values of average S/N ratio for both the elements means that the influential factor ranked 1 is the excitation of the edge elements based on "the larger the better" rule.

Table 7. A response table for a bowtie antenna array.

Element/Level	1	2
1	-30.2381	-62.9008
2	-59.5572	-56.3316
3	-62.7821	-33.3451
$ \eta_{\max} - \eta_{\min} $	32.544	29.5557
Ranking	1	2

The smaller the value of the fitness function and thus the larger the S/N ratio, the closer the results to the desired nulls. The ideal fitness value 0 implies that the results obtained are optimized to attain the desired response. The desired pattern is obtained after 25 iterations with

Table 8. Optimized excitations obtained using Taguchi technique to steer nulls to -50° , 50° and 130° for a bowtie patch antenna array.

Element position	1	2	3	4
Amplitude	0.2377	0.7310	0.7310	0.2377
Normalized Amplitude	0.3252	1	1	0.3252

the element excitations optimized to 0.2377, 0.7310, 0.7310 and 0.2377 as listed in Table 8. The elevation gain pattern shown in Fig. 10 presents the effectiveness of Taguchi method with nulls steered exactly at the desired value, *i.e.* 50° , -50° and 130° . The positions of the nulls along with the corresponding null depth levels for isotropic and non-isotropic antenna arrays of rectangular and bowtie patches, attained by applying Schelkunoff polynomial method and Taguchi method for null steering are summarized in Table 9.

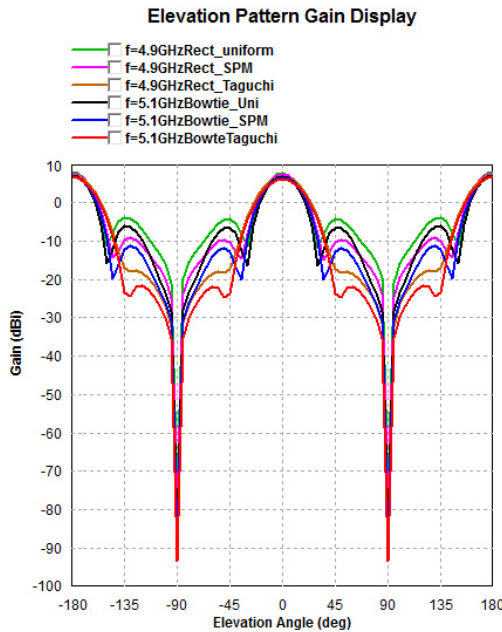


Fig. 10. 2D radiation patterns for 4-element rectangular and bowtie antenna arrays for different excitations.

It can be observed that the SPM gives the same amplitude ratio for all the three arrays irrespective of the elementary radiator, and thus generates the radiation pattern with desired nulls only for the isotropic antenna array, whereas the desired pattern is achieved neither for the rectangular nor bowtie antenna arrays. For Taguchi method however, it can be seen that different amplitude ratios are obtained for the rectangular and bowtie antenna arrays which clearly validates the dependence of the beam pattern on the element factor and hence on the shape of element. The optimized excitations obtained using Taguchi method result in successful steering of the nulls towards the targeted orientation for both the rectangular and bowtie antenna arrays.

In [4] the results computed for a 4-element isotropic antenna array based on the array factor has been applied to a 4-element rectangular patch antenna array. Moreover, the reduction in side

Table 9. Comparison of position and depth of nulls achieved with different techniques for the designed arrays.

Null Positioning Technique	Element Excitations (I ₁ , I ₂)	Elementary radiator	Position and depth of nulls				SLL	No. of iterations
			Null Position					
-	Uniform 1,1	Isotropic	Null Position	60°	-60°	120°	-11	-
			NDL (dB)	-42	-52	-42		
		Rectangular	Null Position	30°	-30°	150°	-11.96	-
			NDL (dB)	-19.21	-19.1	-18.81		
		Bowtie	Null Position	30°	-30°	150°	-13.31	-
			NDL (dB)	-22.59	-22.59	-22.16		
SPM	0.6318, 1.0000	Isotropic	Null Position	50°	-50°	130°	-17	Analytical
			NDL (dB)	-48	-48	-55		
		Rectangular	Null Position	36	-36	144	-16.99	„
			NDL (dB)	-22.17	-22.04	-21.81		
		Bowtie	Null Position	35°	-35°	145°	-18.24	„
			NDL (dB)	-26.68	-26.68	-26.27		
Cuckoo Search Chicken Swarm Algorithm [4]	0.4969, 0.5638	Isotropic	Null Position/ NDL (dB)	Not evaluated			-12.7957	50
		Rectangular					-8.3763	50
Taguchi	0.2097, 0.5906	Rectangular	Null Position	50°	-50°	130°	-24	25
			NDL (dB)	-25.01	-24.95	-24.71		
	0.2377, 0.7310	Bowtie	Null Position	50°	-50°	130°	-28.15	25
			NDL (dB)	-30.9	-30.9	-30.5		

lobe level achieved is greater for the rectangular patch antenna array and bowtie patch antenna array designed in the presented work with Taguchi method, in a much less number of iterations as compared with the array presented in [4].

The maximum NDL for the bowtie antenna array is improved from -22.59 dB to -30.9 dB, when Taguchi method is applied. The suppression of side lobes is also achieved with a significant drop in SLL from -13.31 dB to -28.15 dB for the bowtie antenna array as compared with the designed rectangular array with SLL of -24 dB and the rectangular patch array presented in [4] with maximum achieved SLL of -8.3763 dB. As depicted by S₁₁ curves shown in Fig. 11, the bowtie patch antenna array resonates at 5.1 GHz with a return loss of -20.57 dB whereas the rectangular patch antenna array has a return loss value of -13.72 dB at a resonating frequency of 4.9 GHz. Table 10 enlists other performance parameters of rectangular and bowtie antenna arrays achieved with the optimized excitation. With both antennas resonating at almost the same frequency, the computed results demonstrate that the area of the bowtie patch antenna reduces dramatically to 55 mm² as compared with the rectangular patch antenna with an area of 261.55 mm². The better performance along with a reduced size and maximum gain of 7.6 dB as presented in Table 9 and 10 assure the potential use of the bowtie antenna array in wireless communication systems covering the bands for Wi-Fi and other UWB applications.

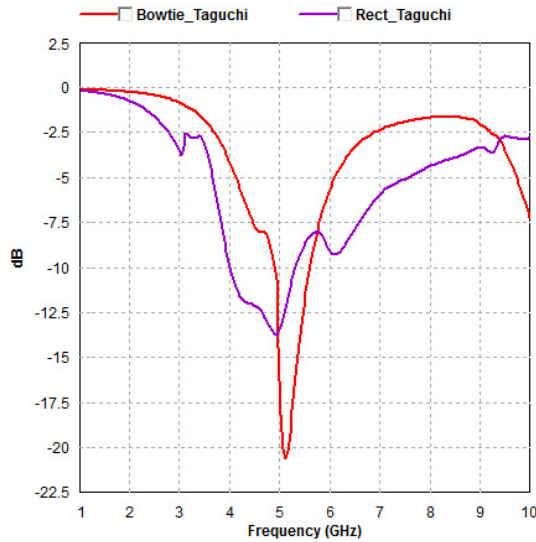


Fig. 11. Comparison of S_{11} for 4-element rectangular and bowtie patch antenna arrays for different excitations.

Table 10. Performance parameters of 4×1 rectangular and bowtie patch antenna arrays attained with the excitations optimized using Taguchi method.

Element	Rectangular	Bowtie
Resonant Frequency (GHz)	4.9	5.1
S_{11} (dB)	-13.50	-20.57
Gain (dBi)	7.2	7.6
Directivity (dBi)	8.5	8.6
Area (mm ²)	261.52	55

5. Conclusion

Taguchi optimization technique inherently considers the element factor and hence performs fast computations, and converges rapidly due to the reduced number of trials based on the orthogonal array design. Satisfactory results of applying Taguchi method for steering nulls towards 50° , -50° and 130° making use of simulation-driven optimization in rectangular and bowtie patch antenna arrays, obtained in 25 iterations demonstrate its validity and efficiency. The 4-bowtie patch antenna array operating at a resonant frequency of 5.1 GHz with S_{11} -20.57 dB shows a size reduction of 80% as compared with the rectangular patch antenna array resonating at 4.9 GHz. There is a considerable reduction in maximum SLL for the bowtie antenna array from -13.31 dB with uniform excitations to -28.15 dB when applied with the excitations computed using Taguchi method, which is better than SLL achieved for the rectangular antenna array. Moreover, the 4-element bowtie patch antenna array results in effective null steering with a gain of 7.6 dB, making it useful for maximizing Wi-Fi performance even in tough and noisy urban conditions polluted with electromagnetic waves.

References

- [1] Berezdivin, R., Breinig, R., Topp, R. (2002). Next-generation wireless communications concepts and technologies. *IEEE Communications Magazine*, 40(3), 108–116.
- [2] Guney, K., Basbug, S. (2008). Interference suppression of linear antenna arrays by amplitude-only control using a bacterial foraging algorithm. *Progress In Electromagnetics Research*, 79, 475–497.
- [3] Guney, K., Durmus, A. (2015). Pattern nulling of linear antenna arrays using backtracking search optimization algorithm. *International Journal of Antennas and Propagation*, 1–10.
- [4] Liang, S., Sun, G. (2017). Sidelobe-level suppression for linear and circular antenna arrays via the cuckoo search–chicken swarm optimization algorithm. *IET Microwaves, Antennas and Propagation*, 11(2), 209–218.
- [5] Saxena, P., Kothari, A. (2016). Optimal pattern synthesis of linear antenna array using grey wolf optimization algorithm. *International Journal of Antennas and Propagation*, 1–11.
- [6] Sun, G., Liu, Y., Li, H., Liang, S., Wang, A., Li, B. (2018). An antenna array side lobe level reduction approach through invasive weed optimization. *International Journal of Antennas and Propagation*, 1–16.
- [7] Recioui, A., Azrar, A., Bentarzi, H., Dehmas, M., Challal, M. (2008). Synthesis of linear arrays with sidelobe level reduction constraint using genetic algorithms. *International Journal of Microwave and Optical Technology*, 3(5), 524–530.
- [8] Koziel, S., Ogurtsov, S. (2015). Rapid design of microstrip antenna arrays by means of surrogate-based optimization. *IET Microwaves Antennas & Propagation*, 9(5), 463–471.
- [9] Koziel, S., Ogurtsov, S., Bekasiewicz, A. (2016). Suppressing sidelobes of linear phased array of microstrip antennas with simulation-based optimization. *Metrol. Meas. Syst.*, 23(2), 193–203.
- [10] Koziel, S., Bekasiewicz, A. (2017). Rapid Design Optimization of Multi-Band Antennas by Means of Response Features. *Metrol. Meas. Syst.*, 24(2), 337–346.
- [11] Babayigit, B., Senyigit, E. (2017). Design optimization of circular antenna arrays using taguchi method. *Neural Computing & Applications*, 28(6), 1443–1452.
- [12] Brintjes, T.M., Kokkeler, A.B.J., Karagiannis, G., Smit, G.J.M. (2015). Shaped pattern synthesis for equispaced linear arrays with non-isotropic antennas. *Proc. IEEE 9th European Conference on Antennas and Propagation*, Lisbon, Portugal, 1–5.
- [13] Guney, K., Onay, M. (2007). Amplitude-only pattern nulling of linear antenna arrays with the use of bees algorithm. *Progress In Electromagnetics Research*, 70, 21–36.
- [14] Mohammed, J.R., Sayidmarie, K.H. (2018). Sensitivity of the adaptive nulling to random errors in amplitude and phase excitations in array elements. *International Journal of Telecommunication, Electronics, and Computer Engineering*, 10(1), 51–56.
- [15] Simons, R.N. (2001). *Coplanar waveguide circuits, components and systems*. New York: John Wiley & Sons.